A novel metamaterial-based microwave sensor design for the characterization of lubricating engine oils and alcohols

K. SANTHOSH KUMAR*, M. GANESH MADHAN
Department of Electronics Engineering, Madras institute of technology. Anna University, Chennai-600044, India

This work introduces a novel metamaterial structure that integrates both square and circular complementary split-ring resonators (CSRRs) in a hybrid arrangement, implemented on a tapered microstrip line. The proposed hybrid metamaterial sensor is employed for the characterization of engine oils and alcohols. The sensor demonstrates a maximum resonance frequency shift of 810 MHz. It achieves a sensitivity of 6.35%, when sensor probe is enclosed with used engine oil. Additionally, it effectively distinguishes different alcohol type's methanol, ethanol, and isopropyl alcohol, based on their unique resonance frequency responses. The simulated performance of the sensor is experimentally verified, confirming its validity. The key novelties of this design include its compact structure, high-quality factor, cost-effective fabrication, and operation at a relatively lower frequency, making it highly suitable for practical industrial sensing applications.

(Received February 24, 2025; accepted October 14, 2025)

Keywords: Microwave sensor, Hybrid CSRR, Engine oil, Alcohol, Sensitivity

1. Introduction

The characterization of liquid dielectrics is a critical task in numerous fields, from chemical engineering to environmental monitoring. Traditional methods often involve complex and destructive techniques. Microwave-based sensors, particularly those utilizing microstrip resonators, offer a promising non-invasive alternative, due to their high sensitivity and simple measurement procedure.

Engine oil lubricates automobile parts for smooth operation. Over time, engine oil loses its lubricating properties. Therefore, it is essential to regularly check the quality of the engine oil and replace it with fresh engine oil, periodically.

Methanol (CH_3OH) is a globally significant chemical with applications in LCD screens, paints, pharmaceuticals, and the automotive industry [1]. As an oxygenated hydrocarbon, methanol is also utilized in fuel cells and internal combustion engines, offering the advantage of reduced nitrogen oxide emissions compared to more complex hydrocarbon fuels. Ethanol (CH_3CH_2OH) finds extensive use in fuels, alcoholic beverages, chemical solvents, and cosmetics. Another versatile alcohol, isopropyl alcohol (C_3H_8O), is a key component in medicine, fuel additives, and ink printing. Given the broad range of industrial applications for these alcohols, their comprehensive characterization has become a crucial area of study. Recently, microwave based liquid sensors have become popular. In [2], a microstrip patch sensor was designed to detect the ratio of ethanol in wines and isopropyl alcohol in disinfectants. These kinds of planar structures have lower sensitivity and Q factor. A rectangular waveguide cavity tuned for TE_{101} mode has been reported [3], where liquid samples are injected into the thermoplastic capillary tubes with 0.5 mm and 1 mm radii. In [4], Microstrip patch antenna coated with single-walled carbon nanotubes was investigated, to improve the sensitivity. Metamaterial based sensors have been implemented for material sensing applications. References [5,6], reported a microwave sensor design for characterizing liquids using a complementary split ring resonator (CSRR) and a split ring resonator (SRR). An asymmetric coplanar strip-fed stepped impedance resonator coupled with an SRR was designed for engine oil and fuel quality detection [7]. A two-port microwave sensor design based on the substrate integrated waveguide was reported to detect water contaminants in diesel [8]. A hexagonal-shaped CSRR [9] is excited using a microstrip line with a two-port configuration for non-invasive monitoring of blood glucose levels. A submersible sensor designed for liquid characterization using monopole antennas coupled with an SRR was reported, but the sensor area is larger. Moreover, it is based on two port topology and focused on higher dielectric constant liquids [10]. A single SRR element is created near the microstrip line and the liquid under test is placed at the open end of the SRR [11]. In our previous work [12], a microwave sensor was designed using a microstrip patch cavity antenna to determine the engine oil quality and its levels. It is an open cavity, over which a radiator is fixed, requiring a stringent measurement procedure. In [13], a sensor operating at a frequency of 11.56 GHz was reported. The generation and processing of high frequencies are complex in the case of sensor development. In [14], multiple circular CSRR-based sensor to measure the permittivity and dielectric loss of liquid, was reported. A hollow glass tube is placed at centre of the rings for measurement of the dielectric constant of the liquid samples. In this research [15], a metamaterial-based sensor utilizing split square ring resonators was

developed to operate within the X-band, for liquid characterization. The proposed sensor is used to sense transformer oil quality, methanol purity, and olive oil adulteration. A resonance frequency shift of approximately 70 MHz, between clean (unused) and contaminated transformer oils (used), was realised. Similarly, when distinguishing between olive oil and corn oil, the sensor exhibited a frequency shift of about 40 MHz. But this sensor exhibited lower frequency shift and less sensitivity. Another research work [16], presents the design and analysis of a compact metamaterial (MTM) based star-shaped split-ring resonator (SRR) enclosed in a square. A sensor sensitivity of 0.92 with a frequency shift of 760 MHz for adulteration is identified. But this sensor is characterised by lower quality factor i.e. 149. In another study [17], the sensor is not compact, because of it is lower operating frequency, two port topology and lower sensitivity. In [18], a metameterial-based split ring type of sensor structure is realized by using a microstrip transmission line. The frequency range is set as 2.5GHz–4 GHz. This design layout is formed by a nested split ring resonator (SRR) and transmission line. The resonant frequencies for 4%, 30 %, and 35% humidity rates of samples are equal to 3.35 GHz, 3.19 GHz, and 3.20GHz respectively. In Ref. [19], X-band metamaterial approaches have been reported for motor-oil quality monitoring. It is a chiral metamaterial sensor with square and circular resonators on an IS680 substrate, where resonance-frequency shifts of 40 MHz (S_{11}) and 30 MHz (S_{22}), between fresh and 10000 km-aged oil, have been observed. The disadvantage of this sensor is that it operates in X band frequency and the frequency shifts are less.

As observed from the state-of-the-art designs, most of the literature on microwave sensors for characterizing liquids, uses either circular or square metamaterial unit elements in different configurations. To improve the electric field interaction with the sample, dielectric tubes were used to hold the sample under test, which is cumbersome for filling and removing the sample. Only very few designs are submersible, however, they also have some limitations.

Hence, to overcome the above drawbacks, a single port, submersible microwave sensor with enhanced sensitivity is developed using a metamaterial structure. Even though submersible, tapered structure, square and circular CSRR shaped fluidic sensors are reported individually earlier, this proposed structure introduces a hybrid square and circular CSRR in a tapered substrate, which is submersible. Further, the sensor design comprises of two square CSRR units and one circular CSRR unit. This arrangement combines the advantages of tapered structure as well as hybrid CSRR, for better sensing characteristics and is compact in nature. Moreover, the structure is capable of sensing engine oils and alcohols, which have varied dielectric values. The design is fabricated and experimentally tested for its characteristics. Moreover, the sensor is compact in nature.

2. Metamaterial based sensor and sensing principle

2.1. Sensor structure

The proposed microwave sensor in Fig.1 (a) is a single-port structure, which is loaded with the two square CSRR units and a circular CSRR, which implements a metamaterial structure, at the flared end of the microstrip line. This sensor design is based on a Roger RO4360G2 substrate with a dielectric constant of 6.4 and a loss tangent of 0.0038. The sensor has a substrate thickness (h) of 0.8 mm and a copper thickness (t) of 0.035 mm. A frequency domain solver in CST-MWS software is used to optimize the sensor parameters.

We use a tapered transmission line to match impedance and reduce reflections; this tapered structure has its characteristic impedance gradually varying and helps to match the load.

The impedance of the tapered structure can be expressed as follows,

$$Z(z) = Z_1 + \left(\frac{Z_2 - Z_1}{L}\right) z$$

where, $Z(z)$ is the characteristic impedance at z.

$Z_1$is the impedance at $z = 0$

$Z_2$is the impedance at $z = L$

L is the total length of the tapered section, $z$denotes the distance along the tapered section.

To obtain a better interaction of the liquid sample with the electric field, two squares and one circular CSRR unit element are loaded near the open end of the flared microstrip line. This optimized structure is identified based on parametric study, which is detailed in the subsequent section III. The sensing area comprising the CSRR units, is immersed in the liquid under test (LUT). The dimensions of the square, circular CSRR units are illustrated in Fig. 1(b) and sensor design parameters are shown in Table 1.

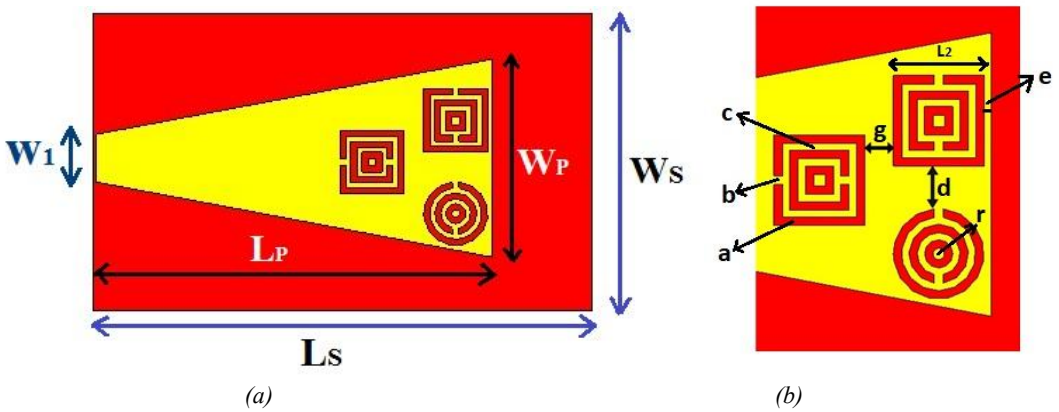

(a) *(b)*

Fig. 1. (a) Geometry of the proposed sensor; (b) Detailed dimensions of the CSRR structures (colour online)

Table 1. Optimized geometric parameters of the designed sensor

Parameter	Value (mm)	Parameter	Value (mm)	Parameter	Value (mm)
L_P	20	L_2	3.20	G	1.00
W_P	10	a	0.30	R	1.60
L_S	25	b	0.30	E	0.25
W_S	15	c	0.25		
W_1	2.50	d	1.50		

2.2. Microwave sensor theory

The proposed metamaterial-based sensor, which has a planar form, can be analyzed using the resonant perturbation method. In this approach, the liquid sample under test, encompasses the CSRR units. Based on the electromagnetic field interaction with the liquid sample, the resonance frequency of the structure is altered. The resonance frequency depends on $\bar{E}$, $\bar{H}$, ε, μ, and the test liquid volume. These parameters change due to the introduction of LUT over the sensing area and lead to shift in the resonance frequency.

2.3 Equivalent circuit

An equivalent quasistatic lumped circuit model [20] of the proposed sensor is shown in Fig.2 (a), where R_1 and L_1 are associated with the tapered patch signal loss, inductance, respectively. C_1, and C_2 are the capacitances, G_1, and G_2 are the conductance's formed between the tapered patch and the ground. L_R, and C_R are the equivalent inductance and capacitance of two square CSRR units, and a circular CSRR unit. L_R, and C_R are the parameters that control the sensor resonant frequency under loaded and unloaded conditions. Moreover, multiple CSRR's are advantageous than single CSRR, for improving the quality factor of the sensor [21]. The hybrid CSRR etched beneath the microstrip line is modelled as a series LC resonator magnetically coupled to the line. The total inductance combines the current loop paths of the square and circular CSRR sections, while the net capacitance is dominated by the slot gaps of the square and circle CSRR section and the electric field is fringing into the liquid under test (LUT).

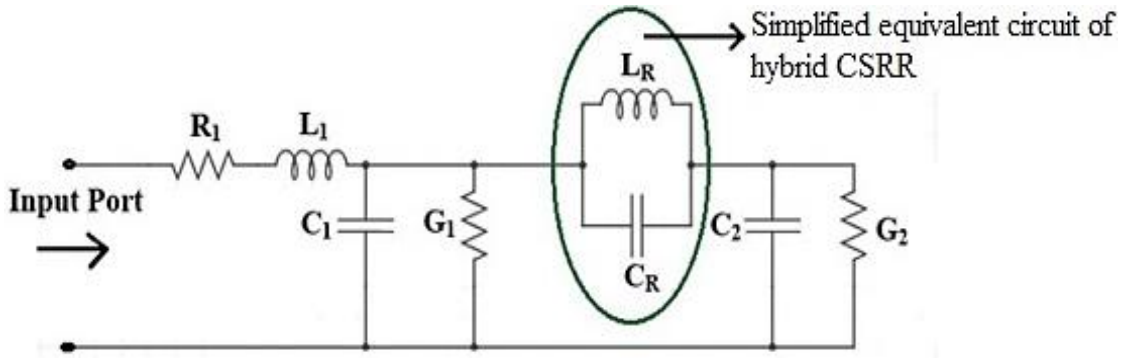

(a)

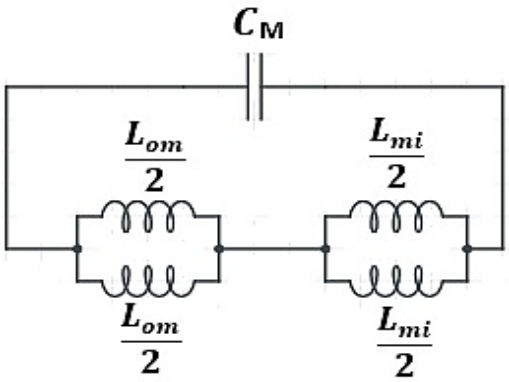

(b)

Fig. 2. (a) Equivalent circuit model of the proposed sensor; (b) Equivalent circuit representation of the CSRR unit

$$f_0 = \frac{1}{2\pi\sqrt{L_M C_M}} \quad (1)$$

$$Where\ L_M = \left[\frac{L_{om}}{4} + \frac{L_{mi}}{4}\right]$$

$$Q = R\sqrt{\frac{C_M}{L_M}} \quad (2)$$

where, C_M and L_M are the equivalent capacitance, inductance of the CSRR unit respectively. R models the loss due to the resistance of the CSRR. At resonance, the reactance due to capacitance (C_M) of the unit element becomes equal to that of the inductance (L_M).

The square, and circular CSRR unit elements are represented by a parallel LC circuit as shown in Fig. 2 (b) [22], where, L_{om}, and L_{mi} in the equivalent circuit represent the inductance between concentric rings of hybrid CSRR structures. Here o, m, and i are the notations used for the outer, middle and inner rings respectively. When the sensor is excited by a time-varying electromagnetic field, its resonance frequency depends on the structural dimensions i.e. a, b, and c, r, L_2. The resonance frequency (f_0), and Q factor of the sensor are defined by equations (1), and (2) [23].

3. Parametric analysis

Parametric analysis is carried out to determine the optimal dimensions of the CSRR elements, as indicated in Fig. 3(a). The S_{11} characteristics of a square CSRR (Fig. 3(b)), for different lengths (L) with a constant split gap (S_g) of 0.3 mm, resulted in a change in resonant frequency (f_r), which is inversely proportional to the length of a square CSRR. Furthermore, we observed a change in the resonance frequency by varying the split gap (S_g), for a constant length (L) of 3.2 mm, as shown in Fig. 3(c). A split gap of 0.3 mm is found to provide an optimal resonant frequency, and reflection coefficient. For brevity, the parametric analysis of a square CSRR located close to the open end of a flared microstrip line alone is included, since, the same dimension is used for the design of other CSRR unit elements.

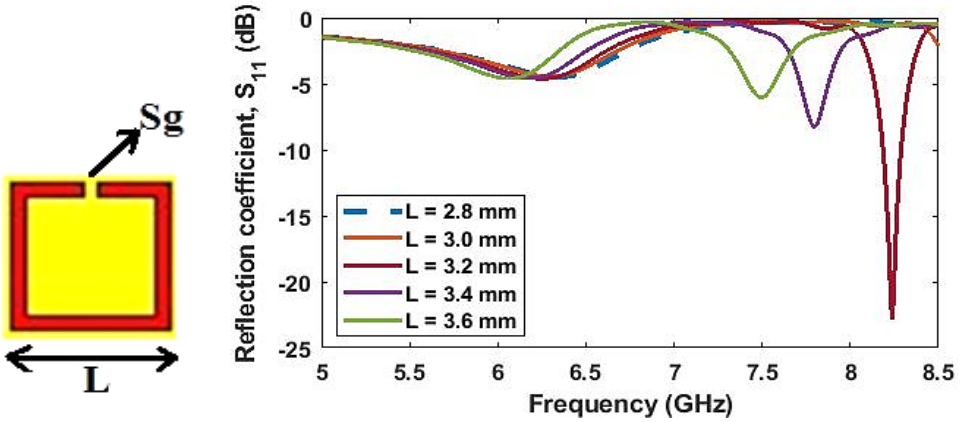

(a)

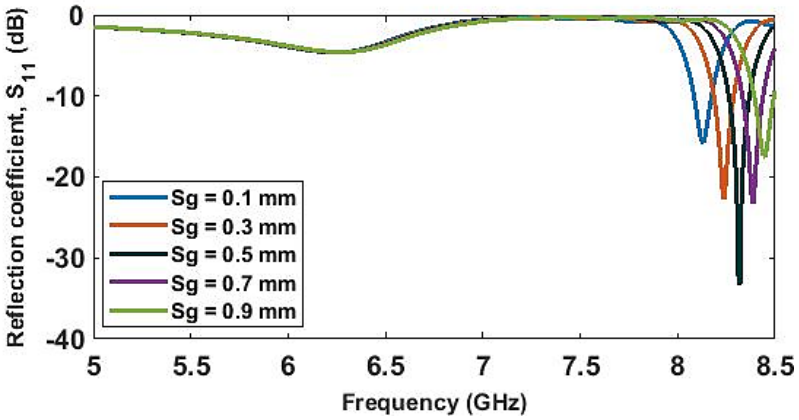

(b)

Fig. 3. (a) Geometrical parameters of the CSRR considered for analysis, (b) S_{11} characteristics corresponding to different lengths (L) of the CSRR, (c) S_{11} characteristics for varying split gaps (S_g) of the CSRR (colour online)

4. Results and discussion

4.1. Simulation

The proposed submersible sensor with metamaterial based on hybrid CSRR is better than the conventional CSRR design in terms of higher Q factor. This results in improved sensitivity even with a smaller volume (20 ml) of liquid sample being tested. The effect of engine oils and alcohols were examined with the developed sensor, whose simulated reflection coefficient (S_{11}) plots are shown in Fig. 5.

The simulated electric field strengths for air, fresh and used engine oils are shown in Fig.6. In the case of the unloaded condition, (air medium) a maximum electric field of 105 dB (V/m) is found to be concentrated at the flare end and CSRR units, which leads to an improved quality factor of 235, along with a small form factor. The presence of oils altered the field, as expected and indicated in Fig. 6 (b) and (c).

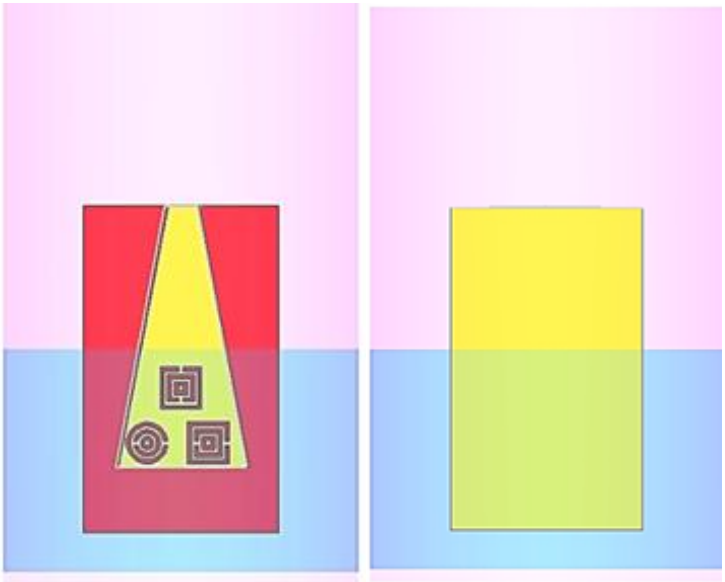

(a) *(b)*

Fig. 4. Simulation model of the proposed sensor integrated with a beaker, where the sensing area is immersed in the liquid under test, (a) Front view, (b) Back view (colour online)

The tapered design achieves intense electric field localization, which translates to markedly higher sensitivity for dielectric characterization. While non-tapered structures offer fabrication simplicity for narrowband applications, our findings conclusively establish that tapered metamaterial sensors are the indispensable architecture for advanced, high-precision sensing applications to get higher sensitivity. A gradual impedance tapering increases the electric-field concentration in the sensing region of hybrid sensor, reduces reflection at the feed transition, and improves the quality factor (Q-factor), when compared with an untampered microstrip. Moreover, this tapered geometry provides stronger electromagnetic coupling to the test liquid due to a wider sensing area without sacrificing

compactness, and lower insertion loss. Hence, it results in an improved resonance shift for incremental change in dielectric constant.

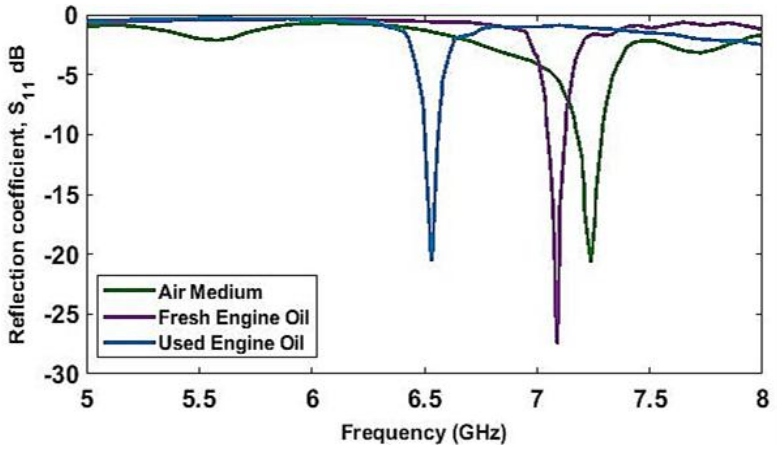

(a)

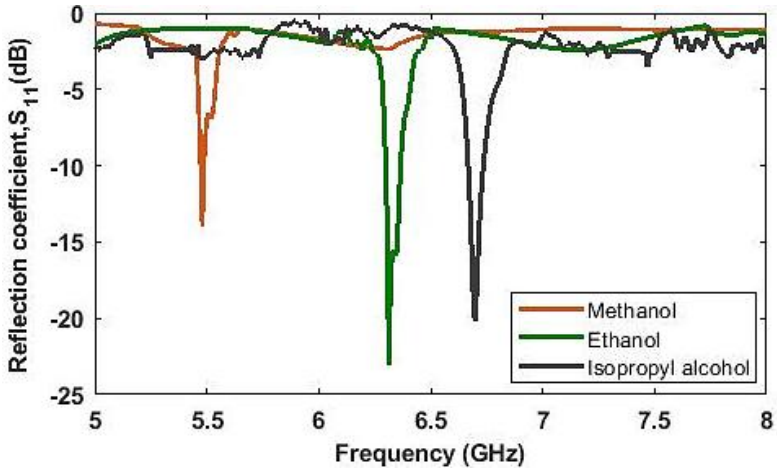

(b)

Fig. 5. S_{11} characteristics of the proposed sensor, (a) Air and with engine oils, and (b) Alcohols (colour online)

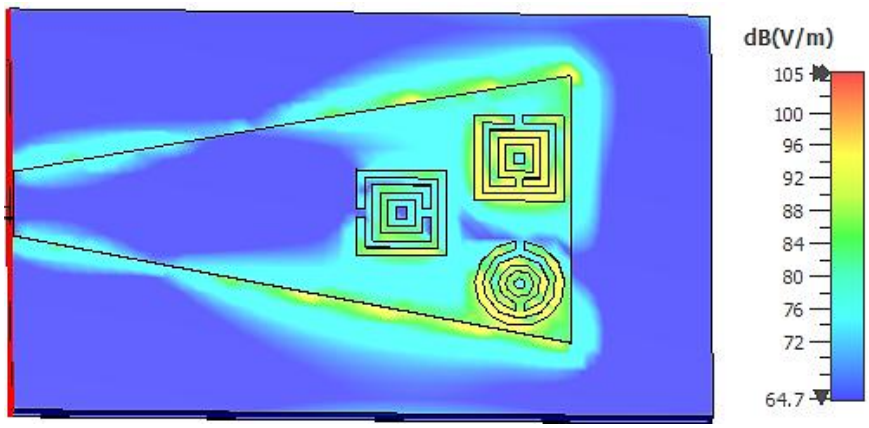

(a)

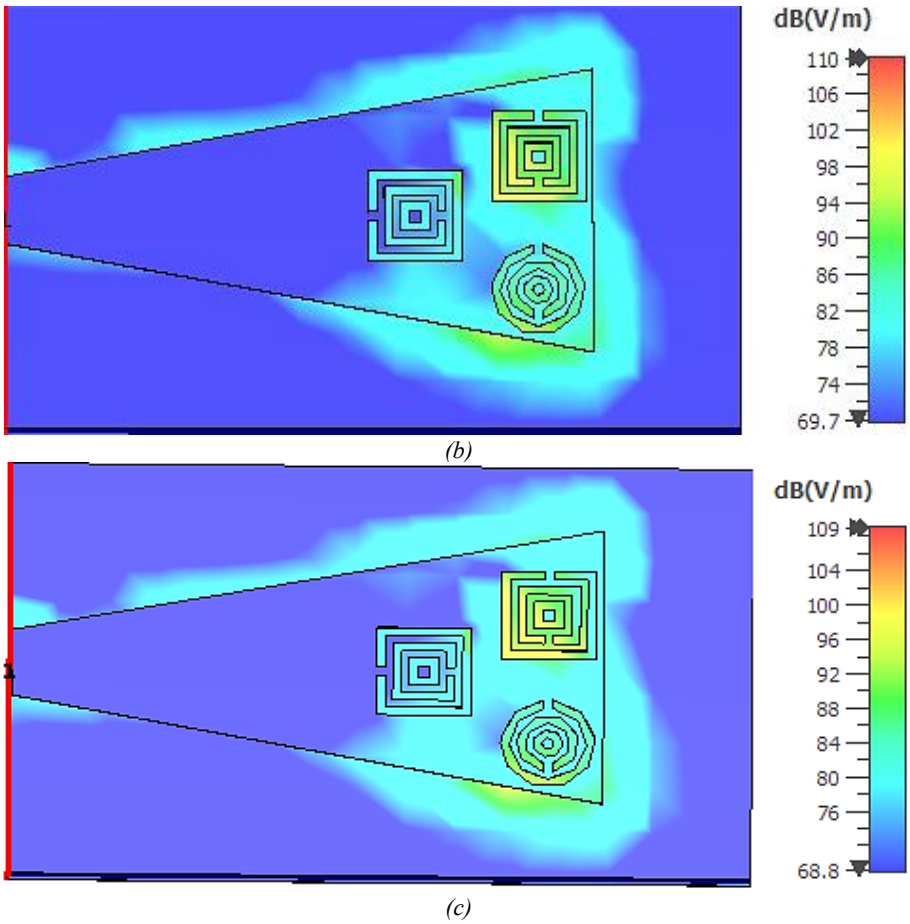

Fig. 6. Electric field distribution of the sensor in different media, (a) Air medium, (b) Fresh engine oil, (c) Used engine oil (colour online)

4.2. Experiment

To validate the effectiveness of the proposed metamaterial sensor, the same design is fabricated and scattering parameter of the sensor is measured using antenna analyzer (R & S, Model ZVH-8). The fabricated sensor and measurement set up are shown in Fig. 7. Initially, the dielectric constants of the engine oil samples were measured using a dielectric probe kit 8070E, PNA-E8361C. The dielectric constants of the fresh and used engine oils were found as 2.32 and 2.74, respectively. Prior to commencing measurements with the network analyzer, a full calibration procedure was performed to eliminate system errors. For each measurement test, 20 mL of the oil sample was placed in a clean polypropylene beaker, and the fabricated sensor was immersed in the liquid under test (LUT), until the CSRR unit elements were completely submerged, as illustrated in Fig. 4. All experiments were conducted under controlled ambient conditions at a room temperature of 28 °C. To avoid cross-contamination, a fresh beaker was used for each sample, and any residual oil on the sensor surface was carefully removed using lint-free cotton swabs. To ensure measurement repeatability and improve accuracy, each test was repeated three timesand the best response is obtained. Comparison of the simulated and measured reflection coefficients (S_{11}) is shown in Fig. 8. In case of the unloaded condition, resonance frequencies of the simulated and measured results are 7.30 GHz and 7.32 GHz respectively. A deviation of 20 MHz is attributed to the fabrication tolerances. Furthermore, in case of alcohols, laboratory reagent samples have been used. The simulated and measured results are found as 7.30 GHz and 7.32 GHz, respectively. Furthermore, in case of alcohols, laboratory reagent samples have been used for measurement, whereas ideal dielectric constants have been used in the simulation. This may have resulted in deviation between the simulation and experimental results. The results for various LUTs are shown in Table 2.

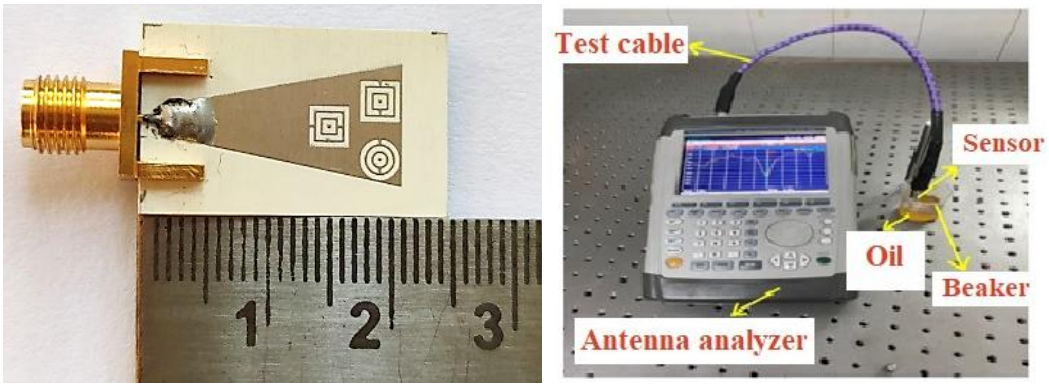

Fig. 7. (a) Prototype of the proposed sensor, (b) Measurement setup (colour online)

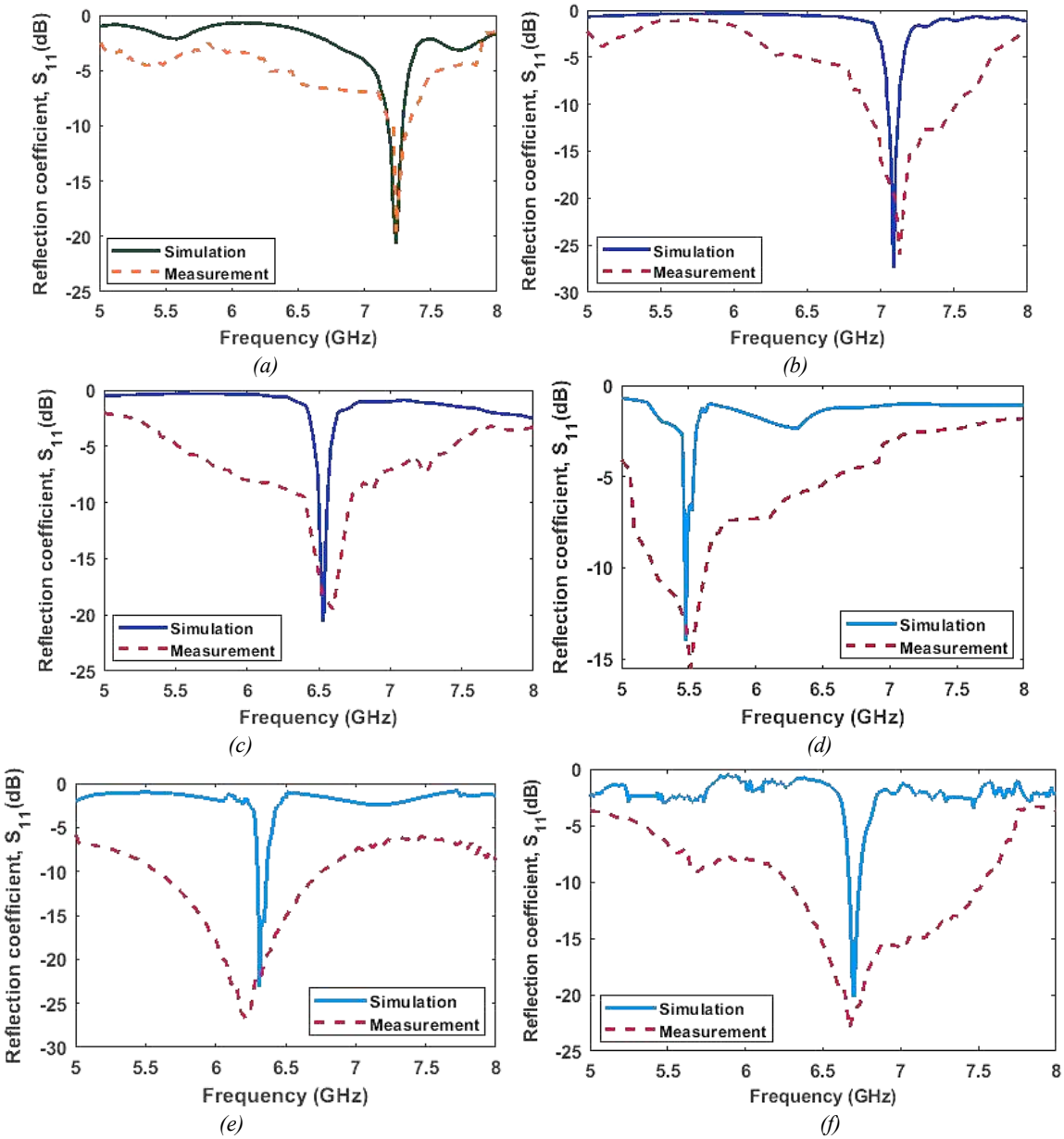

Fig. 8. S_{11} characteristics of the proposed sensor under different mediums: (a) Air, (b) Fresh engine oil, (c) Used engine oil, (d) Methanol, (e) Ethanol, and (f) Isopropyl alcohol (colour online)

Table 2. Measured and simulated results of the proposed sensor for various liquid samples

LUT	Relative Permittivity (ε_r)	Resonant frequency f_r (GHz)		Absolute Error (GHz) (f_{Msr}- f_{Sim})	Reflection coefficient S_{11} (dB)	
		Measurement	Simulation		Measurement	Simulation
Air	1.00	7.32	7.27	0.05	-19.00	-20.80
Fresh engine oil	2.32	7.02	7.00	0.02	-25.00	-27.05
Used engine oil (5000 km)	2.74	6.51	6.50	0.01	-18.00	-20.12
Methanol	32.70	5.51	5.47	0.04	-15.35	-13.85
Ethanol	24.50	6.21	6.32	0.11	-26.72	-22.70
Isopropyl alcohol	17.90	6.70	6.72	0.02	-22.98	-20.10

When engine oil is introduced into the sensing region of the hybrid CSRRs, the resonant frequency decreases, as described by equation (1). This shift is caused by an increase in the effective capacitance of the sensor, which results from the higher permittivity of the liquid under test. For fresh engine oil, the resonant frequency decreases from 7.32 GHz (unloaded condition) to 7.02 GHz, corresponding to a frequency shift of 300 MHz. In the case of used engine oil (after 5000 km run), the resonant frequency decreases from 7.32 GHz to 6.51 GHz, resulting in a larger shift of 810 MHz. This indicates that the used engine oil evinces an additional frequency shift of 510 MHz, compared to fresh oil. The greater reduction in resonant frequency is attributed to changes in the dielectric properties of the engine oil due to continuous use, aging and contamination. Similar to the engine oils, characterization of alcohol samples such as methanol, ethanol and isopropyl alcohol [24] was also carried out using the fabricated sensor.

A strong correlation was observed between the simulated and measured resonant frequencies, with an average absolute error of 0.04 GHz (Average relative error is 0.58%, i.e. it is the ratio of absolute error to the simulation value).

We infer that, the resonant frequencies for both engine oils and alcohols are relatively close, even though the alcohols have significantly high dielectric constant value. The electromagnetic field interaction for both cases is different, since engine oil has less electrical conductivity, as it is primarily composed of hydrocarbon molecules, which do not readily carry electrical conduction. However, in the case of alcohols, electric conduction is present to some extent due to the polar hydroxyl (-OH) groups in these molecules. Hence, it is observed that the electrical properties of the liquids have a significant impact on the capacitance and inductance of the CSRR units, thus leading to a change in the resonant frequency, as identified by the sensor.

In general, the response of CSRR structures should not linearly depend on dielectric value of liquids, as per theoretical equation (1). where the capacitance value decides the resonant frequency. The effective capacitance of the CSRR structure includes the dielectric constant of Sensor substrate, air medium and loaded test sample. When the sensor is submersed, the electric field distribution is non uniform, it means electric field does not penetrate into entire the liquid uniformly. This is quantified by filling factor (η) in eq.3, which denotes the effective dielectric constant [20].

$$\varepsilon_{eff} = \left(\eta.\varepsilon_{liquid}\right) + [(1-\eta).(\varepsilon_{substrate} + \varepsilon_{air})] \quad (3)$$

Typical η is 0.1 to 0.3, for planar resonators.

Several studies have reported the influence of temperature on the dielectric properties of liquids. In Ref. [25], it was shown that the dielectric constant of engine oil decreases with increasing temperature. As temperature rises, molecules gain additional thermal energy, leading to enhancements in their random motion. This thermal agitation disrupts the orderly alignment of induced dipoles along the applied electric field, thereby reducing the net polarization. Similarly, in Ref. [26] demonstrated that the dielectric constant of solvents decreases as temperature increases. In this work [27], a comparable trend was observed for mineral and mixed synthetic oils, where elevated temperature resulted in lower dielectric constant values.

Based on the literature, it can be concluded that both engine oils and alcohols exhibit a reduction in dielectric constant with increasing temperature. According to equation (1), a decrease in permittivity reduces the capacitance of the resonator structure, thereby causing an upward shift in resonant frequency.

The fresh and used engine oils, as well as alcohols, can be differentiated based on the resonance frequency of the sensor. However, when liquids have same dielectric constants, the sensor may resonate at nearly the same frequency. In such cases, distinctions can be made by other electrical parameters such as conductivity, loss tangent, etc.

In addition to temperature effects, contamination also plays a significant role in altering the dielectric behaviour of engine oil. When contaminated with wear particles, soot, oxidation products, or moisture, the effective dielectric constant of engine oil generally increases. This occurs because these contaminants are more polarizable than the base hydrocarbon molecules, thereby enhancing the overall dielectric response of the liquid [28]. This variation leads to

decrease in the resonant frequency of the sensor. It is clear that, in order to properly classify the liquids, the ambient temperature shall be maintained and the contamination in liquids have to be considered during the measurement.

4.3. Sensitivity and quality factor analysis

The dielectric sensitivity (*S*) of the antenna sensor is a parameter that indicates the efficiency of the devised sensor, and the same can be found using the relation in equation (4) [29].

$$S = \frac{\Delta f}{\Delta \varepsilon} = \frac{f_{ru} - f_{rl}}{\varepsilon_{ru} - \varepsilon_{rl}} \quad (4)$$

$$\Delta f = \left| f_{air} - f_{\mathrm{LUT}} \right| \text{ and } \Delta \varepsilon = \left| 1 - \varepsilon_{\mathrm{LUT}} \right|$$

where Δf is the resonance frequency shift, $\Delta \varepsilon$is the variation of the permittivity with a loaded dielectric sample. ε_{ru}, and ε_{rl} are the relative permittivities of the unloaded (air medium), loaded sample (engine oil) andf_{ru}, and f_{rl}, are the corresponding resonant frequencies. We observed maximum dielectric sensitivities of 465 MHz/ε_r, and 75 MHz/ε_r for the used engine oil and isopropyl alcohol respectively. Analytically, the sensitivity percentage of a sensor can be expressed in terms of the change in resonant frequency due to the relative permittivity of the LUT, by using equation (5) [30].

$$S = \frac{f_{air} - f_{sample}}{f_{air}\,(\varepsilon_{rl} - 1)} \times 100 \quad (5)$$

Here, f_{air} represents the resonant frequency when the sensor is unloaded and f_{sample} refers to the resonant frequency when the sensor is subjected to LUTs. The quality factor is another important factor of the sensor, for characterizing the dielectric liquids. A sensor that reports a high Q factor is able to characterize LUTs with high resolution and less ambiguity. The quality factor (Q) calculated for the proposed sensor is based on the following equation (6), which in turn depends on the electrical properties of the surrounding medium [31].

$$Q = \frac{f_0}{f_{3dB}} \quad (6)$$

wheref_0 is the resonance frequency and f_{3dB} is the 3 dB bandwidth measured at $S_{11,\,\mathrm{min.}}$ For the unloaded case, the proposed sensor provides a Q factor is 235.Regarding sensitivity and specificity, more detailed analysis is required, which we propose to work in future.

4.4. Performance comparison with state-of-the-art sensors

To evaluate the performance of the proposed hybrid CSRR-based sensor, its characteristics were compared with previously reported microwave sensors in Table.3. The comparison highlights key parameters such as sensor substrate type, resonant frequency, quality factor, dielectric sensitivity, and submergibility.

From the analysis, we observe that, most works employed either SRR or CSRR structures operate in the lower GHz range (1–3 GHz), with quality factors ranging from 37 to 130 and dielectric sensitivities generally below 3%. In few works [34,35],[38,39], the sensors were designed using FR-4-based substrates and demonstrated cost-effectiveness, but suffered from relatively low sensitivity and poor Q-factors, due to higher dielectric losses. While [34] achieves higher frequency of operation but its sensitivity (0.53%) is lower. In the proposed sensor, the design balances both metrics effectively. Furthermore, many reported sensors were not submersible, limiting their direct liquid measurement capability. In contrast, the proposed sensor, designed on Rogers RO4360G2 substrate, operates at a higher frequency of 7.32 GHz with an exceptionally high-quality factor of 235, thereby ensuring sharper resonance and improved dielectric liquid detection accuracy. In the proposed sensor, the hybrid CSRR configuration enhances the electromagnetic field confinement, resulting in significantly higher dielectric sensitivity, measured as 6.35% for used engine oil and 0.78% for methanol.

Table 3. Comparison of the proposed sensor with existing literature on microwave sensors

Ref. work	Substrate	Sensor Structure	Operating frequency (GHz)	Q -factor	Dielectric Sensitivity S (%)	Submersible
[17]	Rogers AD1000	Double SRR	1.84	130	3.04	Yes
[32]	Rogers RT6002	CSRR	1.91	-	0.44	No
[33]	Rogers RO4350	MCSRR	1.61	-	0.62	No
[34]	FR-4	AESRR	10.5	-	0.53	No
[35]	FR-4 & PDMS	Round slot	2.68	37	1.87	No
[36]	Rogers 4350B	OCSRR	2.35	-	0.88	No
[37]	Rogers 5880	Metamaterial	2.60	-	0.27	No
[38]	FR-4	CSRR	2.40	45	0.21	No

Ref. work	Substrate	Sensor Structure	Operating frequency (GHz)	Q -factor	Dielectric Sensitivity S (%)	Submersible
[39]	FR-4	CSRR	1.20	120	0.62	No
This work	Rogers RO4360G2	Hybrid CSRR	7.32	235	Used engine oil (6.35) Methanol (0.78)	Yes

5. Conclusion

This study introduces a novel metamaterial-based tapered microstrip sensor incorporating a hybrid complementary split-ring resonator (CSRR) configuration consisting of two square CSRRs and one circular CSRR unit, specifically designed for the characterization of engine oils and alcohols. The proposed microwave sensor exhibits enhanced sensitivity, operating at 7.32 GHz with a high-quality factor of 235. Featuring a single-port structure, which facilitates direct immersion in the liquid under test (LUT). Experimental characterization has been conducted for fresh and used engine oils, as well as methanol, ethanol, and isopropyl alcohol within the C-band frequency range. The sensor demonstrates excellent capability in differentiating fresh versus used engine oil and classifying alcohol types. Moreover, its compact size, ease of fabrication, and reusability make it a promising candidate for industrial applications involving real-time monitoring and dielectric characterization of various liquids, including industrial dielectric liquids and edible oils. The present study did not include a systematic evaluation of temperature variation; this will be addressed in future work to validate the sensor's robustness under real-world temperature variations.

Acknowledgements

The authors would like to acknowledge AICTE, New Delhi, for providing financial assistance to carry out this research work under Quality Improvement Programme (QIP) scheme vide Lr.No.QIP/Ph.D./Admn./AR1 and the authors are also thankful to Department of Electrical Engineering, IIT Kanpur, Uttar Pradesh for aiding measurement of dielectric constants of engine oils.

Conflict of interest

The authors declare no conflict of interest for this paper.

References

[1] Sebastian Verhelst, James WG Turner, Louis Sileghem, JeroenVancoillie, Progress in Energy and Combustion Science **70**, 43 (2019).

[2] A. Karatepe, O. Akgol, Y. I. Abdulkarim, S. Dalgac, F. F. Muhammadsharif, H. N. Awl, L. Deng, E. Unal, M. Karaaslan, L. Heng, S. Huang, PLoS One **15**(5), e0232460 (2020).

[3] G. Gennarelli, S. Romeo, M. R. Scarfì, F. Soldovieri, IEEE Sensors Journal **13**(5), 1857 (2013).

[4] W. Becari, D. B. R. Rodrigues, H. E. M. Peres, Current Nano Science **13**, 254 (2017).

[5] M. S. Boybay, O. M. Ramahi, IEEE Transactions on Instrumentation and Measurement **61**(11), 3039 (2012).

[6] M. Schueler, C. Mandel, M. Puentes, R. Jakoby, IEEE Microwave Magazine **13**(2), 57 (2012).

[7] R. Moolat, M. Mani, A. P. Viswanathan, M. Pezholil, International Journal of RF and Microwave Computer Aided Engineering **32**(5), e23095 (2022).

[8] A. M. Loconsole, V. V. Francione, V. Portosi, O. Losito, M. Catalano, A. Di Nisio, F. Attivissimo, F. Prudenzano, Applied Sciences **11**(21), 10454 (2021).

[9] A. E. Omer, G. Shaker, S. Safavi-Naeini, Hamid Kokabi, Georges Alquié, Frédérique Deshours, Raed M. Shubair, Scientific Reports **10**(1), 15200, (2020).

[10] E. Reyes-Vera, G. Acevedo-Osorio, M. Arias-Correa, D. E. Senior, Sensors **19**(8), 1936 (2019).

[11] Withawat Withayachumnankul, Kata Jaruwongrungsee, Adisorn Tuantranont, Christophe Fumeaux, Derek Abbott, Sensors and Actuators A: Physical **189**, 233 (2013).

[12] Kunde Santhosh Kumar, A. Bavithra, M. Ganesh Madhan, Materials Today Proceedings **66**, 3446 (2022).

[13] N. K. Tiwari, S. P. Singh, M. J. Akhtar, IEEE Microwave and Wireless Components Letters **29**(2), 164 (2019).

[14] C. Wang, X. Liu, Z. Huang, S. Yu, X. Yang, X. A. Shang, Sensors **22**(5), 1764 (2022).

[15] Bakir, Mehmet, Muharrem Karaaslan, Faruk Karadag, Sekip Dalgac, Emin Ünal, Oğuzhan Akgöl, Applied Computational Electromagnetics Society Journal (ACES) **5**(1), 799 (2019).

[16] M. A. Khalil, W. H. Yong, T. Batool, Ahasanul Hoque, Lo Yew Chiong, Hui Hwang Goh, Tonni Agustiono Kurniawan, Mohamed S. Soliman, Mohammad Tariqul Islam, Scientific Reports **15**, 2283 (2025).

[17] G. Galindo-Romera, F. Javier Herraiz-Martínez, M. Gil, J. J. Martínez-Martínez, D. Segovia-Vargas, IEEE Sensors Journal **16**(10), 3587 (2016).

[18] Ş. Dalgaç, M. Furat, M. Karaaslan, O. Akgöl, F. Karadağ, M. Zile, M. Bakir, Journal of Electromagnetic Waves and Applications **34**(18),

2488 (2020).
[19] Şekip Dalgaç, Faruk Karadağ, Mehmet Bakir, Oğuzhan Akgöl, Emin Ünal, Muharrem Karaaslan, Transactions of the Institute of Measurement and Control **43**(7), 1640 (2021).
[20] D. M. Pozar, Microwave Engineering, Hoboken, New Jersey: Hamilton Printing, Wiley & Sons, 2021.
[21] F. Bilotti, A. Toscano, L. Vegni, IEEE Transactions on Antennas and Propagation **55**(8), 2258 (2007).
[22] J. D. Baena, Jordi Bonache, Ferran Martín, R. Marques, Francisco Falcone, Txema Lopetegi, Miguel Laso, Joan J. García-García, Ignacio Gil, Maria Flores Portillo, Mario Sorolla Ayza, IEEE Transactions on Microwave Theory and Techniques **53**, 1451 (2005).
[23] J. Bonache, M. Gil, I. Gil, J. Garcia-Garcia, F. Martin, IEEE Microwave and Wireless Components Letters **16**, 543 (2006).
[24] https://depts.washington.edu/eooptic/linkfiles/dielectric_chart%5B1%5D.pdf, dielectric constant of common solvents, University of Washington
[25] Marco Frediani, Guido Giachi, Luca Rosi, Piero Frediani, Microwave heating, Usha Chandra ed., IntechOpen, 181 (2011).
[26] G. D. P. Mahidhar, A. Somasundaram Karthikeyan, R. Sarathi, N. Taylor, H. Edin, IET Science, Measurement and Technology **14**(9), 704 (2020).
[27] H. Lizhi, K. Toyoda, I. Ihara, Journal of Food Engineering **88**(2), 151 (2008).
[28] https://www.machinerylubrication.com/Read/226/dielectric-constant-oil-analysis.
[29] A. Salim, S. Lim, Sensors **16**, 1802 (2016).
[30] S. Kayal, T. Shaw, D. Mitra, Appl. Phys. A **126**(1), 13 (2020).
[31] M. U. Memon, S. Lim, Sensors **18**, 143 (2018).
[32] A. Ebrahimi, J. Scott, K. Ghorbani, IEEE Transactions on Microwave Theory and Techniques **67**(10), 4269 (2019).
[33] H.-Y. Gan, W.-S. Zhao, Q. Liu, D.-W. Wang, L. Dong, G. Wang, W.-Y. Yin, IEEE Sensors Journal **20**(11), 5876 (2020).
[34] Y. Cao, K. Chen, C. Ruan, X. Zhang, Sensors and Actuators A: Physical **331**, 112869 (2021).
[35] X. Han, Y. Zhou, X. Li, Z. Ma, L. Qiao, C. Fu, Sensors **22**, 6410 (2022).
[36] J. Yu, G. Liu, Z. Cheng, Y. Song, M. You, IEEE Sensors Journal **22**, 21489 (2022).
[37] M. Abdolrazzaghi, M. Daneshmand, A. K. Iyer, IEEE Transactions on Microwave Theory and Techniques **66**, 1843 (2018).
[38] A. Buragohain, A. T. T. Mostako, G. S. Das, IEEE Sensors Journal **21**, 27450 (2021).
[39] A. Javed, A. Arif, M. Zubair, M. Q. Mehmood, K. Riaz, IEEE Sensors Journal **20**, 11326 (2020).

*Corresponding author: santhoshkumarkunde@mitindia.edu